

UC San Diego

UC San Diego Previously Published Works

Title

Crystal structure of the chemokine receptor CXCR4 in complex with a viral chemokine

Permalink

<https://escholarship.org/uc/item/9pt8n3ft>

Journal

Science, 347(6226)

ISSN

0036-8075

Authors

Qin, Ling
Kufareva, Irina
Holden, Lauren G
[et al.](#)

Publication Date

2015-03-06

DOI

10.1126/science.1261064

Peer reviewed



Published in final edited form as:

Science. 2015 March 6; 347(6226): 1117–1122. doi:10.1126/science.1261064.

Crystal structure of the chemokine receptor CXCR4 in complex with a viral chemokine[§]

Ling Qin^{1,*}, Irina Kufareva^{1,†,*}, Lauren G. Holden^{1,*}, Chong Wang², Yi Zheng¹, Chunxia Zhao¹, Gustavo Fenalti², Huixian Wu², Gye Won Han^{3,4}, Vadim Cherezov³, Ruben Abagyan¹, Raymond C. Stevens^{3,4,†}, and Tracy M. Handel^{1,†}

¹University of California, San Diego, Skaggs School of Pharmacy and Pharmaceutical Sciences, La Jolla, CA 92093, USA

²Department of Integrative Structural and Computational Biology, The Scripps Research Institute, 10550 North Torrey Pines Road, La Jolla, CA 92037, USA

³Department of Chemistry, Bridge Institute, University of Southern California, Los Angeles, CA 90089, USA

⁴Department of Biological Sciences, Bridge Institute, University of Southern California, Los Angeles, CA 90089, USA

Abstract

Chemokines and their receptors control cell migration during development, immune system responses, and in numerous diseases including inflammation and cancer. The structural basis of receptor:chemokine recognition has been a long-standing unanswered question due to the challenges of structure determination for membrane protein complexes. Here we report the crystal structure of the chemokine receptor CXCR4 in complex with the viral chemokine antagonist vMIP-II at 3.1 Å resolution. The structure revealed a 1:1 stoichiometry and a more extensive binding interface than anticipated from the paradigmatic two-site model. The structure helped rationalize a large body of mutagenesis data, and together with modeling provided insights into CXCR4 interactions with its endogenous ligand CXCL12, its ability to recognize diverse ligands, and the specificity of CC and CXC receptors for their respective chemokines.

Introduction

The chemokine receptor CXCR4 controls cell migration during immune surveillance and development of the cardiovascular, hematopoietic, and central nervous systems (1–3). Like

[§]This manuscript has been accepted for publication in Science. This version has not undergone final editing. Please refer to the complete version of record at <http://www.sciencemag.org/>. The manuscript may not be reproduced or used in any manner that does not fall within the fair use provisions of the Copyright Act without the prior, written permission of AAAS.

[†]Correspondence to: thandel@ucsd.edu, stevens@usc.edu, ikufareva@ucsd.edu.

*Equal contributors

Supplementary content:

Materials and Methods

Figs. S1 to S4

Tables S1 to S3

References (41–56)

many other chemokine receptors (CKRs), CXCR4 contributes to inflammatory diseases and cancer (4, 5). It also functions as one of two co-receptors that facilitate entry of HIV into host immune cells (6). Despite the importance of CXCR4 and CKRs in general, structural insights into CKR:chemokine recognition have been limited to NMR studies of chemokines with peptides derived from CKR N-termini (7–9). This is partly due to the challenges of structure determination for full-length membrane proteins and their complexes.

Here, we present the structure of CXCR4 in complex with vMIP-II, a CC chemokine encoded by Kaposi's sarcoma-associated herpesvirus. vMIP-II functions as a broad-spectrum antagonist of many human CKRs (10) and helps the virus to escape the host immune response (11). We chose vMIP-II for structural studies because it is a high affinity antagonist of CXCR4 (IC₅₀ 6–15 nM (10, 12)), and as a ligand for both CC and CXC chemokine receptors, was expected to provide insight into ligand recognition specificity.

Design of an irreversible CXCR4:vMIP-II complex

Despite high affinity in membranes, the CXCR4:vMIP-II complex was insufficiently stable in detergent to justify crystallization trials. We therefore employed a strategy that utilizes disulfide trapping to generate an irreversible complex (13, 14). Coexpression of pairs of single cysteine mutants of CXCR4 and vMIP-II was expected to result in spontaneous formation of a disulfide bond if the disulfide was compatible with the native geometry of the CKR:chemokine complex. Guided by 3D models of CXCR4:chemokine complexes (14), 37 cysteine mutant pairs were designed and for each pair, the abundance of disulfide-trapped complexes was evaluated (15). These pairs included seven N-terminal cysteine mutants of vMIP-II that were systematically coexpressed with two CXCR4 cysteine mutants, D97^{2.63}C or D187^{ECL2}C (superscript denotes Ballesteros-Weinstein index (16, 17) for helical domain residues; ECL stands for extracellular loop). Of all mutant pairs analyzed, CXCR4(D187C) coexpressed with vMIP-II(W5C) formed the highest percentage of trapped complex (Fig. 1A). It also showed an unfolding temperature of 63°C (Fig. 1B), which is 4 to 14°C higher than other mutant combinations, and excellent monodispersity when analyzed by size exclusion chromatography (Fig. S1). By comparison, the mutant pair with the second highest melting temperature, CXCR4(D187C):vMIP-II(H6C) (59°C), was produced in significantly lower yield and showed lower monodispersity, despite the adjacent position of the vMIP-II cysteine (Fig. S1). CXCR4(D97C) formed little or no covalent complex with any of the seven vMIP-II mutants tested (Fig. 1A, B). The observed sensitivity of several biophysical properties of the complex to precise cysteine placement suggests specificity of the disulfide-trapping approach and supports compatibility of the D187C:W5C disulfide bond with the native complex geometry. We therefore selected CXCR4(D187C):vMIP-II(W5C) for crystallization in lipidic cubic phase (LCP) (18), and determined the structure at 3.1 Å resolution. Data collection and refinement statistics are shown in Table S1.

Overall complex geometry

In complex with vMIP-II, CXCR4 possesses the typical seven TM helical topology. Whereas previous dimeric structures of CXCR4 suggested that chemokines might bind receptors in a 2:1 CKR:chemokine stoichiometry (19, 20), the present structure demonstrates

that the stoichiometry is 1:1, in agreement with a recent study (14). The chemokine interacts via its globular core with the receptor N-terminus (chemokine recognition site 1, CRS1 (21)) and via its N-terminus with the receptor TM pocket (CRS2) (Fig. 1C). Clear electron density is observed for the entire chemokine N-terminus, including the CXCR4(D187C):vMIP-II(W5C) disulfide bond, which adopts a favorable geometry (Fig. 1D). Residues 1–22 of the receptor are not visible in the density, consistent with the moderate stability of the CRS1 interaction between CXCR4 and vMIP-II as suggested by disulfide-trapping experiments (Fig. S2) and prior mutagenesis studies (12).

Molecular interactions between CXCR4 and vMIP-II

The CXCR4:vMIP-II interaction is mediated by an extensive (1330 Å²) contiguous interface, with every residue in the chemokine N-terminus and N-loop (1-LGASCHRPDKCCLGYQ-16) contacting the receptor (Fig. 2, Table S2). Although parts of the interface can be classified as CRS1 or CRS2, the absence of a distinct boundary prompted introduction of an intermediate region, CRS1.5 (Fig. 2A, B). The CRS1 interaction involves CXCR4 N-terminal residues 23-SMKEP-27 packing against the chemokine N-loop (residues 13-LGYQ-16) and its third β-strand (β₃, residues 49-QVC-51) (Fig. 2C, D, Table S2). This interaction continues towards CRS1.5 where receptor residues 27-PCFRE-31 bind to chemokine residues 8-PDKCC-12 (Fig. 2C, D) and form an anti-parallel β-sheet. In CRS2, the chemokine N-terminus makes hydrogen bonds to receptor residues D97^{2.63}, D262^{6.58} and E288^{7.39} and numerous van der Waals packing interactions (Fig. 2C, D, Table S2). Most of the interacting CXCR4 residues are known determinants of either vMIP-II binding (Table S3) or CXCL12 binding and activation (22–26). The dominant role of the vMIP-II N-terminus is supported by the fact that an isolated vMIP-II(1–21) peptide binds CXCR4 with appreciable affinity (190 nM (12) vs 6–15 nM for wild-type vMIP-II (10, 12)), which is dramatically reduced by mutations L1A, R7A, and K10A (27) (Table S3). Notably, a W5A mutation has only a moderate effect (27). Disulfide-trapping studies also support the role of the chemokine N-loop (Fig. S2).

Comparison of CXCR4:vMIP-II with previous structures

The conformation of the observed part of the receptor N-terminus differs significantly from previous small-molecule and peptide-bound structures (19), in that it adopts an orientation almost perpendicular to the membrane to form a β-sheet interaction in CRS1.5 with chemokine residues C11–C12 (Fig. 3A, B). To accommodate this change as well as binding of the chemokine N-terminus in the TM pocket, the extracellular half of helix I is laterally shifted outwards by ~2.4 Å, forming an extra α-helical turn and bending at the top (Fig. 3A). ECL2 forms a β-hairpin as in other CXCR4 structures but is more closed onto the binding pocket (Fig. 3A), bringing D181 and D182 of CXCR4 in close proximity with K10 of vMIP-II (Fig. 2C, D).

The binding pocket of CXCR4 is open and negatively charged (Fig. 3C), and can be separated into a major and minor subpocket (28). Similar to the small molecule antagonist, IT1t, the chemokine N-terminus makes the majority of contacts in the minor subpocket and makes polar interactions with D97^{2.63} and E288^{7.39} (Fig. 3C, D). By contrast, the spatial

overlap between the vMIP-II N-terminus and CVX15 is moderate, with common recognition determinants including D187^{ECL2} and D262^{6.58} (Fig. 3C, E). The limited overlap between CVX15 and the chemokine N-terminus may enable the design of modulators that simultaneously occupy the minor and major subpockets; in fact, a series of CXCR4 ligands obtained by grafting the N-terminus of CXCL12 onto a peptide analogue of CVX15 (29) may bind CXCR4 in this manner.

As in five earlier structures (19), CXCR4 forms a dimer in the vMIP-II-bound form (Fig. 4A). The preservation of similar dimerization patterns in all CXCR4 structures (Fig. 4B) suggests possible physiological relevance and is consistent with numerous reports of CXCR4 homo- and heterodimerization in cells ((30) and references therein). The structure also suggests that a receptor dimer can accommodate two monomeric chemokine ligands.

Structure comparisons, bioinformatics, and homology modeling insights into the specificity of CC and CXC chemokine recognition by CKRs

With the exception of atypical CKRs, human CC and CXC chemokines generally pair exclusively with CKRs from the same subfamily. To gain insight into this specificity, as well as the non-canonical pairing of a human CXC receptor (CXCR4) with a viral CC chemokine (vMIP-II), structural and sequence analyses (Fig. S4) were complemented by molecular modeling (15). A complex between CXCR4 and its endogenous CXC chemokine, CXCL12, as well as a complex between vMIP-II and another human CKR, CCR5, were chosen for analysis due to available structural and mutagenesis information.

An initial systematic analysis of chemokine structures revealed conformational differences between CC and CXC motifs of the respective chemokines: while in CC chemokines, this region is straight and forms β -sheet interactions within chemokine dimers, it is bent in CXC chemokines and forms no substantial protein-protein interface contacts (Fig. S4A). This difference is reflected in the CRS1.5 interactions of the structure and the modeled complexes (Fig. 5A–C). In the CXCR4: CXCL12 model (Fig. 5A), the bend directs the chemokine N-terminus towards receptor helices V/VI and enables hydrogen bonding between chemokine R8 (highly conserved as a base in CXC but not CC chemokines, Fig. S4B) and receptor D262^{6.58} (highly conserved as an acid in CXC but not CC CKRs, Fig. S4C). By contrast, in the CCR5: vMIP-II model (Fig. 5C), the straightened conformation of the chemokine CC motif directs the chemokine N-terminus along the receptor N-terminus towards helix I, aided by interactions with receptor K22 in position C+2 (where C is the conserved N-terminal cysteine) and with D276^{7.32}. Notably a base in position C+2 and an acid in position 7.32 are both highly conserved in CC but not CXC CKRs (Fig. S4C). Furthermore, mutation of K22 or D276^{7.32} in CCR5 abrogates binding to vMIP-II, CCL3, and CCL5 (31). Interestingly, both vMIP-II and CXCR4 possess features that are atypical for their respective classes; vMIP-II has three basic residues (H6, R7, K10) in its proximal N-terminus (Fig. S4B) and CXCR4 has a base (R30) at C+2 (Fig. S4C), which may partially explain the unusual coupling between CXCR4 and vMIP-II.

Relevant differences between CC and CXC families are also observed in the predicted CRS1 interactions. The presence of sulfotyrosines sY14 and sY15 (32) in proximity of the

conserved N-terminal cysteine in CCR5 (Fig. S4C) facilitates interactions with basic residues in the vMIP-II N-loop (K17 and R18) and β_2 - β_3 loop (R46 and R48) (Fig. 5C). When evaluated family-wide, high acidity and sulfotyrosine content of the proximal N-terminus are characteristic of CC but not CXC receptors (Fig. S4C), whereas the basic nature of N- and β_2 - β_3 loops distinguishes CC from CXC chemokines (Fig. S4B). It appears therefore, that even when sulfotyrosines in the N-terminus of CXC receptors contribute to chemokine affinity, they do not engage the N- or β_2 - β_3 loops of CXC chemokines. Consistent with this notion, CXCR4 sY21 is predicted to interact with the CXCL12 N-loop- β_1 -strand junction (Fig. 5A) instead of the neutral N- and β_2 - β_3 loops, similar to positions of sulfate groups in multiple CXCL12 structures (33, 34). The cleft defined by the N- and β_2 - β_3 loops of CXCL12 is occupied by the backbone of CXCR4 residues S23-M24, which closely mimic the interaction of a small molecule CXCR4: CXCL12 inhibitor (34). CXCR4 is a rare CXC receptor that possesses a sulfotyrosine in the proximal N-terminus (position C-7, Fig. S4C), which may explain its unique ability to engage a CC chemokine (vMIP-II) via its basic N- or β_2 - β_3 loops. This engagement is further assisted by a 4-residue epitope in the chemokine β_3 -strand that is strictly conserved between vMIP-II (48-RQVC-51) and CXCL12 (47-RQVC-50) and that interacts with receptor D22 and E26 (Fig. 5B), both of which are important for vMIP-II and CXCL12 recognition (23, 26).

The CXCR4:vMIP-II structure can also explain why CXC (35) but not CC (36) chemokines bind and activate their receptors as dimers. CC chemokines dimerize by β -sheet interactions between the straight CC motifs and N-terminal residues (Fig. 6A). This largely coincides with the CRS1.5 interaction in the CXCR4:vMIP-II structure, making it sterically impossible for a CC chemokine to simultaneously bind its dimer partner and a receptor (Fig. 6B). By contrast, CXC chemokines dimerize by their β_1 -strands (Fig. 6C), which are not involved in receptor interactions and therefore compatible with the geometry of the CKR:chemokine complexes (Fig. 6D). This model also suggests that CXC chemokine dimers likely bind to single receptor subunits (Fig. 6E) and not to both subunits in a dimer as previously hypothesized (37).

Modeling-based insights into agonist vs antagonist chemokine binding to CXCR4

CXCL12 can be converted into a potent antagonist of CXCR4 by as little as a single N-terminal amino-acid substitution (P2G) (38). To investigate the basis for this dramatic change in pharmacology, modeling of CRS2 interactions for both CXCL12 and CXCL12(P2G) with CXCR4 was performed. With both chemokine variants, the four distal N-terminal residues were predicted to bind in the minor subpocket of CXCR4 in a manner similar to vMIP-II (Fig. 5D, E). The N-terminal and side-chain amines of chemokine K1 were predicted to form hydrogen bonds to receptor residues D97^{2.63} and E288^{7.39}, respectively, while chemokine residues S4 (in CXCL12) and Y7 (in both CXCL12 and CXCL12(P2G)) hydrogen-bond to D187^{ECL2}. Notably, K1 in CXCL12 and D97^{2.63}, D187, E288^{7.39} in CXCR4 are all critical for receptor interaction and activation (22, 25, 26, 38). In CXCL12, the side-chain of P2 was found in proximity of receptor residue Y116^{3.32} (Fig. 5D) whose direct interaction with agonists is frequently involved in activation of GPCRs

(39). By contrast, due to its greater flexibility and smaller steric volume, the G2-S4 region of CXCL12(P2G) packed differently (Fig. 5E), avoiding interaction with Y116^{3,32} and potentially explaining the inability of CXCL12(P2G) to activate CXCR4. However, because docking was performed with an inactive receptor conformation, further structural studies will be necessary to fully understand activation mechanisms.

Chemokine Receptor Plasticity, Promiscuity and Implications for Drug Design

CXCR4 is remarkable in its ability to recognize multiple unrelated small molecules, peptides, and proteins. While engaging a conserved set of binding determinants, the ligands occupy different regions of the binding pocket due to receptor conformational plasticity involving receptor side-chain and backbone adjustments. Such versatility may allow the receptor to accommodate ligands of different classes including both CC and CXC type chemokines as well as allosteric inhibitors. The growing number of chemokine receptor structures with different ligands opens possibilities for rational design of ligands that have improved inhibition profiles and mechanisms of action.

Supplementary Material

Refer to Web version on PubMed Central for supplementary material.

Acknowledgments

The authors thank H. Zhang and W. Liu for help with X-ray data collection, A. Walker for assistance with manuscript preparation, M. Gustavsson and V. Katritch for valuable discussions and critical reading of the manuscript, M. Chu for assistance with insect cell expression, E. Lolis and J. Murphy for suggesting the use of vMIP-II, T. Kawamura, D. Hamel and K. Wang for assistance with chemokine production. The data in this manuscript are tabulated in the main paper and in the supplementary materials. Atomic coordinates and structure factors have been deposited in the Protein Data Bank with identification code 4RWS.

This work was funded by National Institutes of Health grants R01 GM071872 (RA), U01 GM094612, R01 GM081763 and R21 AI101687 (TMH), and U54 GM094618 (RCS). LGH is supported by 2012 Postdoctoral Fellowship in Pharmacology/Toxicology from the Pharmaceutical Research and Manufacturers of America (PhRMA) Foundation. The General Medical Sciences and Cancer Institutes Structural Biology Facility at the Advanced Photon Source (GM/CA@APS) is supported by the National Cancer Institute (ACB-12002) and the National Institute of General Medical Sciences (AGM-12006).

References and Notes

1. Nagasawa T, et al. Defects of B-cell lymphopoiesis and bone-marrow myelopoiesis in mice lacking the CXC chemokine PBSF/SDF-1. *Nature*. 1996; 382:635. [PubMed: 8757135]
2. Zou YR, et al. Function of the chemokine receptor CXCR4 in haematopoiesis and in cerebellar development. *Nature*. 1998; 393:595. [PubMed: 9634238]
3. Ma Q, et al. Impaired B-lymphopoiesis, myelopoiesis, and derailed cerebellar neuron migration in CXCR4- and SDF-1-deficient mice. *Proc Natl Acad Sci USA*. 1998; 95:9448. [PubMed: 9689100]
4. Koelink PJ, et al. Targeting chemokine receptors in chronic inflammatory diseases: An extensive review. *Pharmacol Ther*. 2012; 133:1. [PubMed: 21839114]
5. Balkwill F. The significance of cancer cell expression of the chemokine receptor CXCR4. *Semin Cancer Biol*. 2004; 14:171. [PubMed: 15246052]
6. Berger EA, Murphy PM, Farber JM. Chemokine Receptors as HIV-1 Coreceptors: Roles in Viral Entry, Tropism, and Disease. *Annu Rev Immunol*. 1999; 17:657. [PubMed: 10358771]

7. Skelton NJ, Quan C, Reilly D, Lowman H. Structure of a CXC chemokine-receptor fragment in complex with interleukin-8. *Structure*. 1999; 7:157. [PubMed: 10368283]
8. Veldkamp CT, et al. Structural Basis of CXCR4 Sulfotyrosine Recognition by the Chemokine SDF-1/CXCL12. *Sci Signal*. 2008; 1:ra4. [PubMed: 18799424]
9. Millard, Christopher J., et al. Structural Basis of Receptor Sulfotyrosine Recognition by a CC Chemokine: The N-Terminal Region of CCR3 Bound to CCL11/Eotaxin-1. *Structure*. 2014; 22:1571. [PubMed: 25450766]
10. Kledal TN, et al. A Broad-Spectrum Chemokine Antagonist Encoded by Kaposi's Sarcoma-Associated Herpesvirus. *Science*. 1997; 277:1656. [PubMed: 9287217]
11. Yamin R, et al. The Viral KSHV Chemokine vMIP-II Inhibits the Migration of Naive and Activated Human NK Cells by Antagonizing Two Distinct Chemokine Receptors. *PLoS Pathog*. 2013; 9:e1003568. [PubMed: 23966863]
12. Zhou N, et al. A Novel Peptide Antagonist of CXCR4 Derived from the N-Terminus of Viral Chemokine vMIP-II. *Biochemistry*. 2000; 39:3782. [PubMed: 10736178]
13. Rosenbaum DM, et al. Structure and function of an irreversible agonist-b2 adrenoceptor complex. *Nature*. 2011; 469:236. [PubMed: 21228876]
14. Kufareva I, et al. Stoichiometry and geometry of the CXC chemokine receptor 4 complex with CXC ligand 12: Molecular modeling and experimental validation. *Proc Natl Acad Sci USA*. 2014; 111:E5363. [PubMed: 25468967]
15. Materials and methods are available as supplementary material on Science Online
16. Ballesteros, JA.; Weinstein, H. *Methods in Neurosciences*. Vol. 25. Academic Press; 1995. Integrated methods for the construction of three-dimensional models and computational probing of structure-function relations in G protein-coupled receptors; p. 366
17. In Ballesteros-Weinstein numbering, the most conserved residue in class A GPCRs is designated x. 50, where x is the transmembrane helix number. All other residues on a given helix are numbered relative to this position, e.g. x.49, x.51 are the flanking residues.
18. Caffrey M, Cherezov V. Crystallizing membrane proteins using lipidic mesophases. *Nat Protoc*. 2009; 4:706. [PubMed: 19390528]
19. Wu B, et al. Structures of the CXCR4 Chemokine GPCR with Small-Molecule and Cyclic Peptide Antagonists. *Science*. 2010; 330:1066. [PubMed: 20929726]
20. Kufareva, I.; Abagyan, R.; Handel, TM. *Chemokines*. Vol. chap 77. Springer; Berlin Heidelberg: 2014. Role of 3D Structures in Understanding, Predicting, and Designing Molecular Interactions in the Chemokine Receptor Family; p. 1
21. Scholten DJ, et al. Pharmacological modulation of chemokine receptor function. *Br J Pharmacol*. 2011; 165:1617. [PubMed: 21699506]
22. Tian S, et al. Distinct functional sites for human immunodeficiency virus type 1 and stromal cell-derived factor 1alpha on CXCR4 transmembrane helical domains. *J Virol*. 2005; 79:12667. [PubMed: 16188969]
23. Brelot A, Heveker N, Montes M, Alizon M. Identification of residues of CXCR4 critical for human immunodeficiency virus coreceptor and chemokine receptor activities. *J Biol Chem*. 2000; 275:23736. [PubMed: 10825158]
24. Våbenø J, Nikiforovich GV, Marshall GR. Insight into the Binding Mode for Cyclopentapeptide Antagonists of the CXCR4 Receptor. *Chem Biol & Drug Design*. 2006; 67:346.
25. Choi WT, et al. Unique ligand binding sites on CXCR4 probed by a chemical biology approach: implications for the design of selective human immunodeficiency virus type 1 inhibitors. *J Virol*. 2005; 79:15398. [PubMed: 16306611]
26. Zhou N, et al. Structural and Functional Characterization of Human CXCR4 as a Chemokine Receptor and HIV-1 Co-receptor by Mutagenesis and Molecular Modeling Studies. *J Biol Chem*. 2001; 276:42826. [PubMed: 11551942]
27. Luo Z, et al. Structure-Function Study and Anti-HIV Activity of Synthetic Peptide Analogues Derived from Viral Chemokine vMIP-II. *Biochemistry*. 2000; 39:13545. [PubMed: 11063591]
28. Roumen L, et al. C(X)CR in silico: Computer-aided prediction of chemokine receptor-ligand interactions. *Drug Discovery Today: Technologies*. 2012; 9:e281. [PubMed: 24990665]

29. Lefrançois M, et al. Agonists for the Chemokine Receptor CXCR4. *ACS Medicinal Chemistry Letters*. 2011; 2:597. [PubMed: 21841963]
30. Stephens, B.; Handel, TM. Chemokine Receptor Oligomerization and Allostery. In: Kenakin, T., editor. *Oligomerization and Allosteric Modulation in G-Protein Coupled Receptors*. Vol. 115. Academic Press; 2013. p. 375chap. 9
31. Navenot JM, et al. Molecular anatomy of CCR5 engagement by physiologic and viral chemokines and HIV-1 envelope glycoproteins: differences in primary structural requirements for RANTES, MIP-1 α , and vMIP-II binding. *J Mol Biol*. 2001; 313:1181. [PubMed: 11700073]
32. Farzan M, et al. Tyrosine sulfation of the amino terminus of CCR5 facilitates HIV-1 entry. *Cell*. 1999; 96:667. [PubMed: 10089882]
33. Murphy JW, et al. Structural and Functional Basis of CXCL12 (Stromal Cell-derived Factor-1 α) Binding to Heparin. *J Biol Chem*. 2007; 282:10018. [PubMed: 17264079]
34. Smith EW, et al. Structural Analysis of a Novel Small Molecule Ligand Bound to the CXCL12 Chemokine. *J Med Chem*. 2014
35. Drury LJ, et al. Monomeric and dimeric CXCL12 inhibit metastasis through distinct CXCR4 interactions and signaling pathways. *Proc Natl Acad Sci USA*. 2011; 108:17655. [PubMed: 21990345]
36. Jin H, et al. The Human CC Chemokine MIP-1 β Dimer Is Not Competent to Bind to the CCR5 Receptor. *J Biol Chem*. 2007; 282:27976. [PubMed: 17644519]
37. Rajasekaran D, et al. A Model of GAG/MIP-2/CXCR2 Interfaces and Its Functional Effects. *Biochemistry*. 2012; 51:5642. [PubMed: 22686371]
38. Crump MP, et al. Solution structure and basis for functional activity of stromal cell-derived factor-1; dissociation of CXCR4 activation from binding and inhibition of HIV-1. *Embo J*. 1997; 16:6996. [PubMed: 9384579]
39. Katritch V, Cherezov V, Stevens RC. Structure-Function of the G Protein-Coupled Receptor Superfamily. *Annu Rev Pharmacol Toxicol*. 2013; 53:531. [PubMed: 23140243]
40. Alexandrov AI, et al. Microscale Fluorescent Thermal Stability Assay for Membrane Proteins. *Structure*. 2008; 16:351. [PubMed: 18334210]
41. Kufareva I, Chen YC, Ilatovskiy AV, Abagyan R. Compound activity prediction using models of binding pockets or ligand properties in 3D. *Curr Top Med Chem*. 2012; 12:1869. [PubMed: 23116466]
42. Cherezov V, et al. Rastering strategy for screening and centring of microcrystal samples of human membrane proteins with a sub-10 μ m size X-ray synchrotron beam. *J R Soc Interface*. 2009; 6:S587. [PubMed: 19535414]
43. Stepanov S, et al. JBluIce-EPICS control system for macromolecular crystallography. *Acta Crystallogr D Biol Crystallogr*. 2011; 67:176. [PubMed: 21358048]
44. Kabsch W. XDS. *Acta Crystallogr D Biol Crystallogr*. 2010; 66:125. [PubMed: 20124692]
45. Otwinowski Z, Minor W. Processing of X-ray Diffraction Data Collected in Oscillation Mode. *Methods in Enzymology*. 1997; 276:307.
46. McCoy AJ, et al. Phaser crystallographic software. *J Appl Crystallogr*. 2007; 40:658. [PubMed: 19461840]
47. Emsley P, Cowtan K. Coot: model-building tools for molecular graphics. *Acta Crystallogr D Biol Crystallogr*. 2004; 60:2126. [PubMed: 15572765]
48. Adams PD, et al. PHENIX: a comprehensive Python-based system for macromolecular structure solution. *Acta Crystallogr D Biol Crystallogr*. 2010; 66:213. [PubMed: 20124702]
49. Abagyan R, Totrov M. Biased probability Monte Carlo conformational searches and electrostatic calculations for peptides and proteins. *J Mol Biol*. 1994; 235:983. [PubMed: 8289329]
50. Ohnishi Y, et al. Crystal Structure of Recombinant Native SDF-1 α with Additional Mutagenesis Studies: An Attempt at a More Comprehensive Interpretation of Accumulated Structure-Activity Relationship Data. *Journal of Interferon & Cytokine Research*. 2000; 20:691. [PubMed: 10954912]

51. Dealwis C, et al. Crystal structure of chemically synthesized [N33A] stromal cell-derived factor 1 α , a potent ligand for the HIV-1 “fusin” coreceptor. *Proc Natl Acad Sci USA*. 1998; 95:6941. [PubMed: 9618518]
52. Kufareva I, et al. Status of GPCR modeling and docking as reflected by community-wide GPCR Dock 2010 assessment. *Structure*. 2011; 19:1108. [PubMed: 21827947]
53. Wong RSY, et al. Comparison of the Potential Multiple Binding Modes of Bicyclam, Monocyclam, and Noncyclam Small-Molecule CXC Chemokine Receptor 4 Inhibitors. *Mol Pharmacol*. 2008; 74:1485. [PubMed: 18768385]
54. Gerlach LO, Skerlj RT, Bridger GJ, Schwartz TW. Molecular interactions of cyclam and bicyclam non-peptide antagonists with the CXCR4 chemokine receptor. *J Biol Chem*. 2001; 276:14153. [PubMed: 11154697]
55. Zhou H, Tai HH. Expression and functional characterization of mutant human CXCR4 in insect cells: role of cysteinyl and negatively charged residues in ligand binding. *Arch Biochem Biophys*. 2000; 373:211. [PubMed: 10620340]
56. Rosenkilde MM, et al. Molecular mechanism of AMD3100 antagonism in the CXCR4 receptor: transfer of binding site to the CXCR3 receptor. *J Biol Chem*. 2004; 279:3033. [PubMed: 14585837]

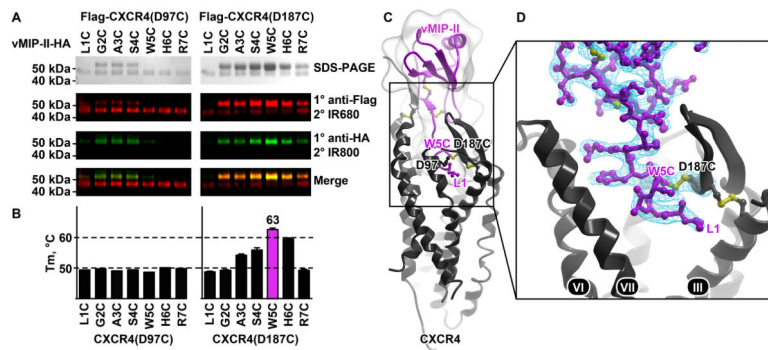


Fig. 1. Design and crystallization of a disulfide-trapped CXCR4:vMIP-II complex. **(A)** Non-reducing SDS-PAGE and Western blot of CXCR4(D97C) (left) and CXCR4(D187C) (right) coexpressed with cysteine mutants of vMIP-II (residues 1–7). Uncomplexed CXCR4 and disulfide-trapped complexes have molecular weights of approximately 45 kDa and 55 kDa, respectively. Band identities were confirmed by Western blot using antibodies against the FLAG and HA tags at the N- and C-termini of CXCR4 and vMIP-II, respectively (2nd and 3rd row). The 55 kDa band was labeled by anti-FLAG and anti-HA antibodies (2nd–4th row); the band at 45 kDa was only labeled by the anti-FLAG antibody (2nd and 4th row). **(B)** Thermal stability of the complexes measured by a CPM assay (40) are shown as mean \pm SEM measurements performed in triplicate. **(C)** Overall structure of the CXCR4:vMIP-II complex (gray:magenta ribbon and transparent mesh). **(D)** Zoomed view of the vMIP-II N-terminus in the CXCR4 pocket showing the CXCR4(D187C):vMIP-II(W5C) disulfide bond. The 2mFo-DFc electron density map around the N-terminus is contoured at 1.0σ and colored blue.

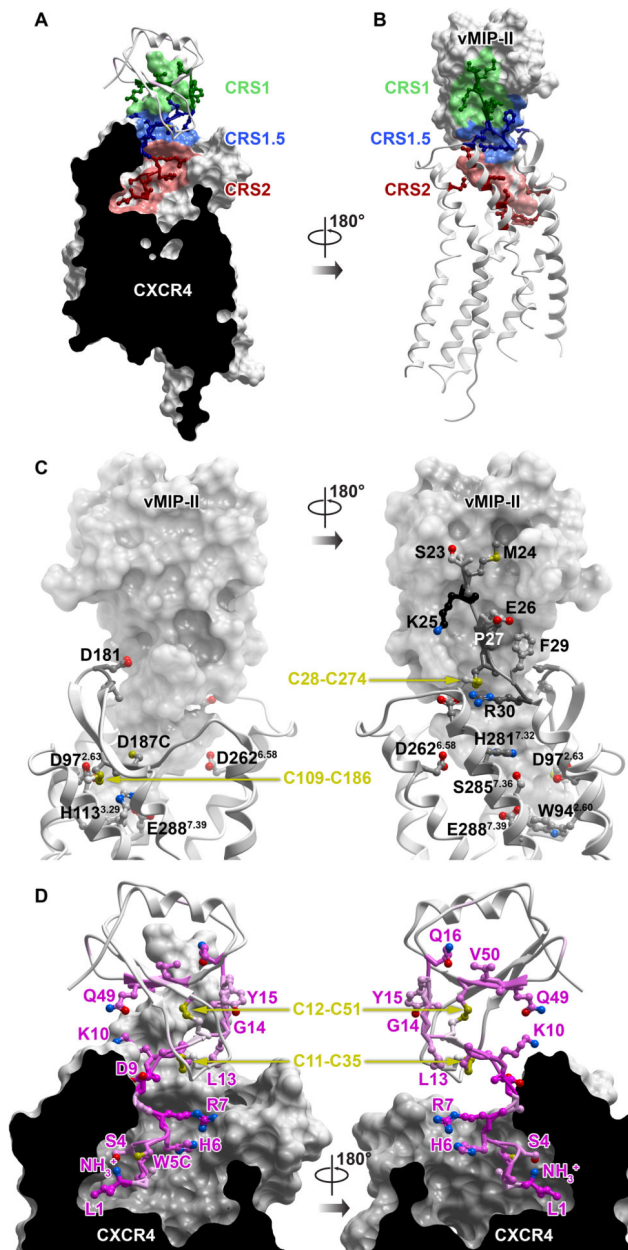


Fig. 2.

Interactions between CXCR4 and vMIP-II. **(A–B)** The interaction is mediated by a contiguous interface containing CRS1 (green), CRS2 (red) and CRS1.5 (blue). **(A)** The receptor is shown as a cut-open surface, the chemokine is shown as a ribbon, chemokine residues making substantial contacts with the receptor are shown as sticks. **(B)** The receptor is shown as a ribbon, receptor residues making substantial contacts with chemokine are shown as sticks, and vMIP-II is shown as a surface mesh. **(C)** Key residues (gray sticks) from CXCR4 (ribbon) that bind vMIP-II (surface representation). **(D)** Key residues (magenta sticks) from vMIP-II (white ribbon) that bind CXCR4 (cut-open surface). Non-

carbon atoms are red (O), blue (N), and yellow (S); carbon stick color intensity is indicative of residue contact strength (Table S2).

Author Manuscript

Author Manuscript

Author Manuscript

Author Manuscript

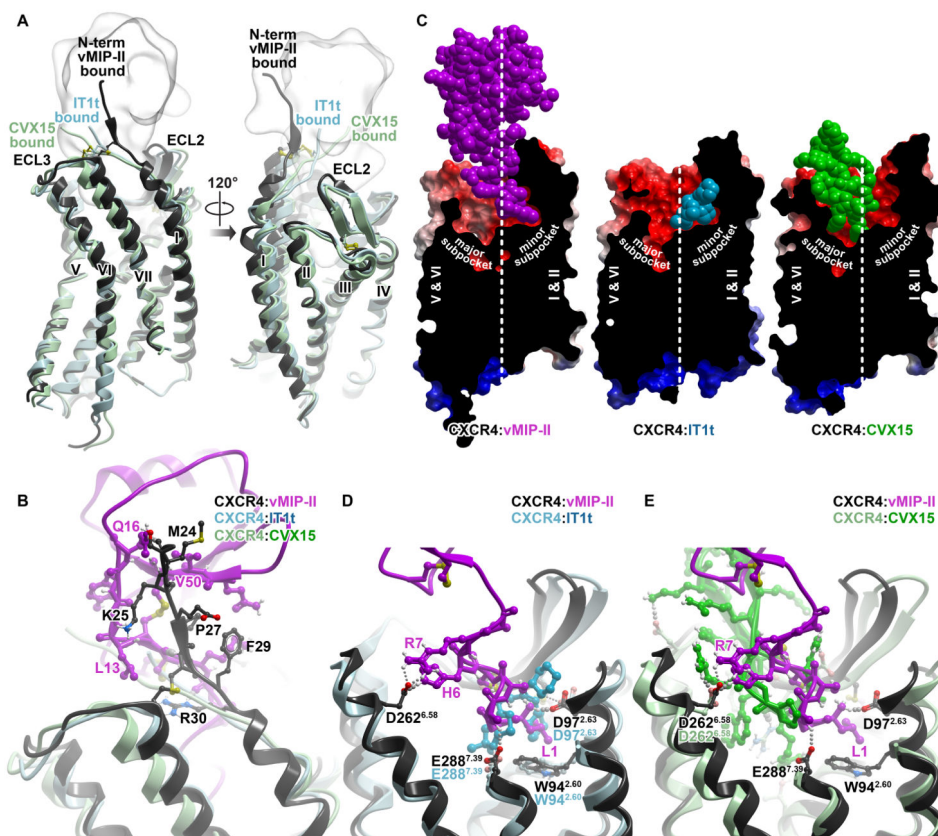


Fig. 3. Comparison between CXCR4:vMIP-II and earlier CXCR4 structures. (A) Overlay of CXCR4 in the vMIP-II complex (gray), the IT1t complex (PDB ID 3ODU; cyan), and the CVX15 complex (PDB ID 3OE0; pale green). vMIP-II is shown as a gray transparent mesh. (B) CRS1 interaction between CXCR4 (gray) and vMIP-II (magenta), in comparison with IT1t-bound (cyan) and CVX15-bound (green) structures. Key residues mediating the CXCR4:vMIP-II interactions are shown as sticks. (C) Binding modes of vMIP-II, IT1t and CVX15 to CXCR4. CXCR4 is shown as a cut-open surface, colored by electrostatic potential; the bound ligands are shown as spheres. The white dotted line represents the boundary between the major and minor subpockets. (D–E) Comparison of CRS2 interactions of vMIP-II (magenta) with IT1t (cyan) and CVX15 (green).

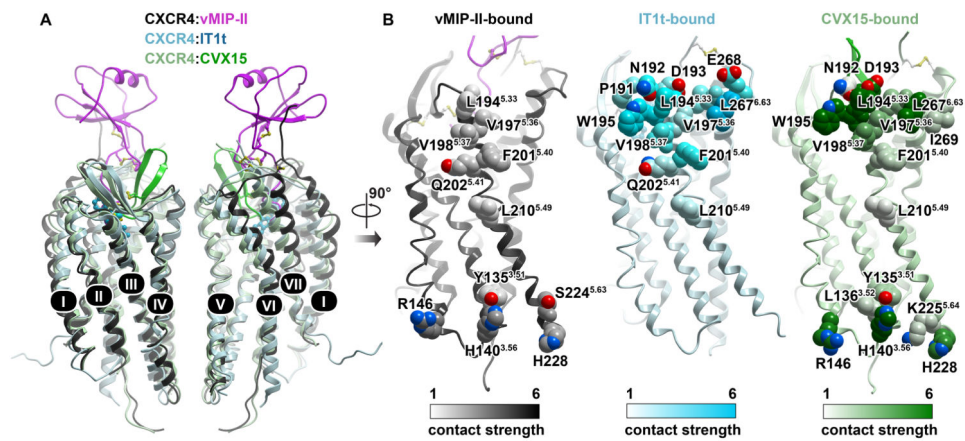


Fig. 4.

Crystallographic dimer of CXCR4:vMIP-II. **(A)** The overall dimer geometry is similar between CXCR4:vMIP-II (gray:magenta), CXCR4:IT1t (PDB ID 3ODU, light cyan:dark cyan), and CXCR4:CVX15 (PDB ID 3OE0, light green:green). **(B)** In all CXCR4 complexes solved thus far, the interaction between two CXCR4 molecules (ribbon) is mediated by the top halves of helix V, with additional contacts provided by either intracellular parts of helices III and V, or the top halves of helix VI (spheres). Views of the dimer interface on one monomer are shown for CXCR4:vMIP-II, CXCR4:IT1t, and CXCR4:CVX15 complexes. Residues that contribute to dimer formation are shown as spheres; color intensities represent contact strength.

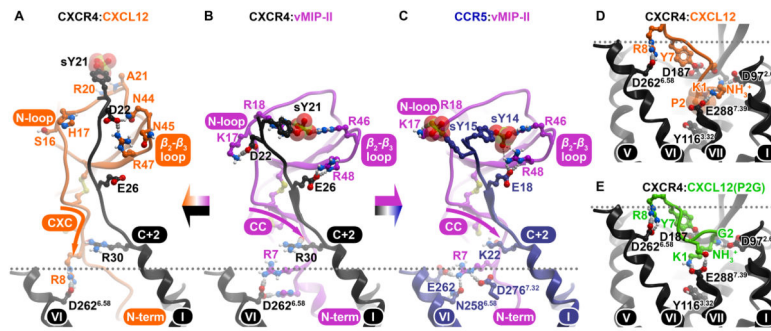


Fig. 5. Molecular models of homologous receptor:chemokine complexes: CXCR4: CXCL12 (**A**, **D**), CXCR4: vMIP-II (**B**), CCR5: vMIP-II (**C**), and CXCR4: CXCL12(P2G) (**E**). Panels **A–C** focus on CRS1 and CRS1.5 interactions while panels (**D–E**) show predicted CRS2 interactions. The dotted line indicates the approximate extracellular membrane-solvent boundary. (**B**) A model of WT CXCR4 sY21-F304 (gray) is built in complex with WT vMIP-II (magenta). Despite the absence of the D187C-W5C disulfide bond, the predicted interactions coincide precisely with those observed in the X-ray structure. vMIP-II W5 provides additional packing interaction with ECL2 of CXCR4. (**A**, **C**) Models of CXCR4: CXCL12 (gray:orange) and CCR5: vMIP-II (navy:magenta). (**D–E**) Models of CXCR4: CXCL12 (gray:orange) and CXCR4: CXCL12(P2G) (gray:green).

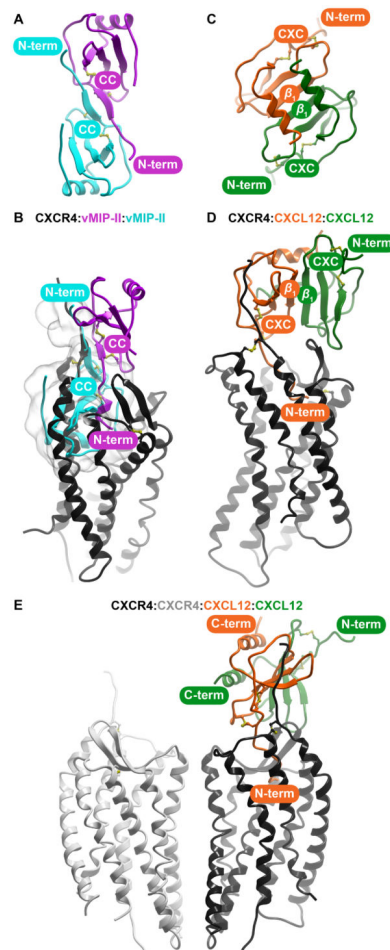


Fig. 6. Implications of the CXCR4:vMIP-II structure for understanding the stoichiometry of receptor:chemokine recognition. **(A)** vMIP-II (shown, PDB ID 2FHT) and other CC chemokine dimers are stabilized by β -sheet formation between the CC region and neighboring residues. **(B)** Superposition of the vMIP-II dimer onto the CXCR4:vMIP-II structure shows that binding of a CC dimer to the receptor is sterically impossible. **(C)** CXCL12 (shown, PDB ID 3GV3) and other CXC chemokine dimers are stabilized by β -sheet formation between their β_1 -strands. **(D)** Superposition of the CXCL12 dimer onto the CXCR4:vMIP-II structure shows that binding of a dimer is feasible. **(E)** If the receptor dimer geometry is relevant, and the vMIP-II orientation is predictive of CXC chemokine binding, CXC dimers do not simultaneously bind both receptors in a dimer.